

**The microwave spectrum of an unstable molecule: Chloro ketene ClHCCO**

M. C. L. Gerry, W. Lewis Bevan, and N. P. C. Westwood

Citation: *The Journal of Chemical Physics* **79**, 4655 (1983); doi: 10.1063/1.445606

View online: <http://dx.doi.org/10.1063/1.445606>

View Table of Contents: <http://scitation.aip.org/content/aip/journal/jcp/79/10?ver=pdfcov>

Published by the [AIP Publishing](#)

---

**Articles you may be interested in**

[Infrared diode laser and microwave spectra and molecular structure of an unstable molecule, FBO](#)

*J. Chem. Phys.* **87**, 2006 (1987); 10.1063/1.453175

[The submillimeterwave spectrum of the HCCO radical](#)

*J. Chem. Phys.* **86**, 4319 (1987); 10.1063/1.451892

[The microwave spectrum of an unstable molecule, HPO](#)

*J. Chem. Phys.* **84**, 1157 (1986); 10.1063/1.450505

[Unstable continuous spectrum in magnetohydrodynamics](#)

*Phys. Fluids* **22**, 1700 (1979); 10.1063/1.862805

[The Methyl Alcohol Molecule and Its Microwave Spectrum](#)

*J. Chem. Phys.* **21**, 1804 (1953); 10.1063/1.1698668

---



# The microwave spectrum of an unstable molecule: Chloroketene ClHCCO

M. C. L. Gerry, W. Lewis-Bevan, and N. P. C. Westwood

Department of Chemistry, The University of British Columbia, 2036 Main Mall, Vancouver, British Columbia, Canada V6T 1Y6

(Received 6 July 1983; accepted 9 August 1983)

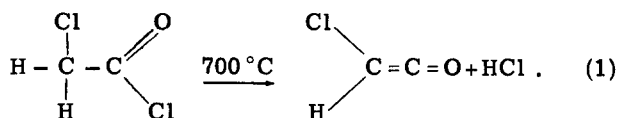
The microwave spectra of four isotopic species of the unstable molecule chloroketene ClHCCO have been observed from the flow pyrolysis of monochloroacetyl chloride and from the pyrolytic reaction of dichloroacetyl chloride with zinc metal. The spectra, which consist only of *b*-type transitions, were observed in the frequency range 26.5–80 GHz. Accurate rotational constants and quartic and sextic centrifugal distortion constants have been obtained for all isotopes. Large numbers of perturbations have been observed in the chlorine quadrupole hyperfine structure; consequently, the complete quadrupole coupling tensor has been evaluated. The dipole moment has been measured. The molecule has been shown to be planar, and a partial  $r_0$  structure has been determined.

## INTRODUCTION

Although ketene  $H_2CCO$  has been the subject of intensive spectroscopic investigation, including its observation as an interstellar molecule,<sup>1</sup> little is known of its substituted derivatives. The monomethyl- and dimethylketenes have been observed by microwave and infrared spectroscopy<sup>2–5</sup> despite their propensity for dimerization. There is, however, a paucity of data on the halogen substituted derivatives. These have been observed as reactive intermediates in solution, undergoing 1,2-cycloaddition with olefins and other unsaturated compounds,<sup>6,7</sup> but it is only recently that monohalo- and dihaloketenes have been observed as discrete molecules in the gas phase using HeI photoelectron spectroscopy (UPS).<sup>8,9</sup> The preparative routes described for detection by UPS parallel those used in the solution work, viz. dehydrohalogenation or dehalogenation of halo-substituted acid chlorides. Both have been used for the microwave observation of chloroketene.

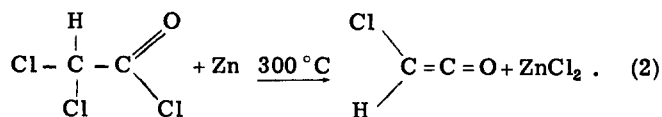
## EXPERIMENTAL METHODS

For the majority of the observations described here, chloroketene was prepared by direct flow pyrolysis of monochloroacetyl chloride in an 8 mm. i.d. quartz tube heated to 700 °C over about 10 cm of its length. The dehydrochlorination may be represented by the equation



Decomposition of the starting material begins at ~500 °C and is complete at 700 °C.

In the other preparation, dichloroacetyl chloride was passed over zinc at 300 °C. The equation for this is



This method has the advantage that a lower temperature is used, and that the only gaseous product is the desired

chloroketene. Its disadvantage is that the zinc is relatively easily poisoned, and often has to be replaced.

Deuterated chloroketene was prepared by pyrolysis of monochloroacetylchloride- $d_2$ ; the latter was prepared from monochloroacetic acid- $d_3$  (MSD isotopes) by treatment with  $\text{PCl}_3$ .

The effluent from the pyrolysis zone was pumped continuously through a 2 m copper X band cell of a conventional 100 kHz Stark modulated spectrometer at a typical pressure of 30 mTorr. HCl was not observed in the frequency range used in this work. All observed lines in the microwave spectrum could be ascribed to chloroketene.

Microwave spectra were obtained for four isotopic species:  $^{35}\text{ClHCCO}$ ,  $^{37}\text{ClHCCO}$ ,  $^{35}\text{ClDCCO}$ , and  $^{37}\text{ClDCCO}$ . They were measured in the frequency regions 26.5–40 and 53–80 GHz. For the former the source was a backward wave oscillator contained in a Hewlett Packard 8400 C microwave spectroscopy source. Frequency doubling using a Space Kom DV-1 doubler permitted extension to the upper range. Estimated measurement accuracies are  $\sim \pm 0.05$  MHz below 40 GHz and  $\sim \pm 0.1$  MHz above 53 GHz.

## OBSERVED SPECTRUM AND ASSIGNMENT

A preliminary calculation of rotational constants using structural data transferred from vinyl chloride<sup>10</sup> and methylketene<sup>3</sup> was used as the basis for prediction of a rigid rotor spectrum for  $^{35}\text{ClHCCO}$ . Predicted values for the chlorine nuclear quadrupole coupling constants  $\chi_{aa}$  and  $\chi_{bb} - \chi_{cc}$  were calculated from the equations of Townes and Dailey<sup>11</sup> using chlorine atomic charges derived from a minimal basis (STO-3G) *ab initio* calculation (GAUSSIAN 70).<sup>12</sup>

The molecule was expected to be a planar near symmetric prolate rotor, probably having both *a*- and *b*-type transitions. Surprisingly, no obvious *a*-type *R* branches were found. Instead a set of *b*-type *Q*-branch transitions ( $J_1, J_{-1} - J_0, J$ ) was quickly identified from its chlorine quadrupole hyperfine patterns, and gave two linear combinations of the rotational constants. To separate the

rotational constants an assignment of  $P$  and  $R$  branches was required; the first transitions to be identified, also from their hyperfine patterns, were of the type  $J-1_{2,J-3}-J_{1,J}$ . Once they had been found, and accurate quadrupole coupling constants had been determined, further  $P$  and  $R$  branches were readily identified and a large number of transitions were assigned by the usual bootstrap procedure, including both rotational constants and centrifugal distortion constants. All observed transitions were  $b$  type. The frequency fit was the chief criterion for assignment, confirmed always by the hyperfine structure. For this isotope 58 rotational transitions up to  $J=74$  were assigned and measured.

A minor refinement of the  $^{35}\text{ClHCCO}$  structural parameters permitted the  $^{37}\text{ClHCCO}$ ,  $^{35}\text{ClDCCO}$ , and  $^{37}\text{ClDCCO}$  rotational constants and line frequencies to be predicted with sufficient accuracy to provide a ready analysis of their observed spectra. For the latter three isotopes,

56, 31, and 38 rotational transitions, respectively, were fitted.

## ANALYSIS OF THE SPECTRA

### Rotational constants and centrifugal distortion constants

To obtain the rotational and centrifugal distortion constants of chloroketene, it was first necessary to account for the hyperfine structure using the chlorine nuclear quadrupole coupling constants obtained as described below. The hypothetical unsplit frequencies were then analyzed using Watson's  $A$ -reduction Hamiltonian in the  $I'$  representation<sup>13</sup>:

$$\mathcal{H} = \mathcal{H}_R + \mathcal{H}_D, \quad (3)$$

$$\mathcal{H}_R = \frac{1}{2}(B+C)J^2 + [A - \frac{1}{2}(B+C)]J_a^2 + \frac{1}{2}(B-C)(J_b^2 - J_c^2), \quad (4)$$

$$\begin{aligned} \mathcal{H}_D = & -\Delta_J J^4 - \Delta_{JK} J^2 J_a^2 - \Delta_K J_a^4 - 2\delta_J J^2 (J_b^2 - J_c^2) - \delta_K [J_a^2 (J_b^2 - J_c^2) + (J_b^2 - J_c^2) J_a^2] + H_J J^6 + H_{JK} J^4 J_a^2 + H_{KJ} J^2 J_a^4 + H_K J_a^6 \\ & + (h_J J^4 + h_{JK} J^2 J_a^2 + h_K J_a^4) (J_b^2 - J_c^2) + (J_b^2 - J_c^2) (h_J J^4 + h_{JK} J^2 J_a^2 + h_K J_a^4). \end{aligned} \quad (5)$$

To account for the observed spectra, rotational constants and both quartic and sextic distortion constants were required. Meaningful values could be obtained for all rotational and quartic constants, but for only a partial set of sextic constants. In particular  $H_{JK}$  and  $h_K$  could not be obtained from the present data, and were constrained to zero. For  $^{35}\text{ClDCCO}$ ,  $h_J$  was also constrained to zero, for the same reason. The derived constants are in Table I. The unsplit line frequencies of the observed transitions are in Table II for the four different isotopes, along with the differences between the observed frequencies and those calculated from the derived constants.

### The chlorine quadrupole coupling tensor

For a planar molecule containing a single quadrupolar nucleus the quadrupole Hamiltonian can be written as follows:

$$\mathcal{H}_Q = \chi_{aa} \phi_{Za}^2 + \chi_{bb} \phi_{Zb}^2 + \chi_{cc} \phi_{Zc}^2 + 2\chi_{ab} \phi_{Za} \phi_{Zb}, \quad (6)$$

where  $\chi_{fg}$  is a quadrupole coupling constant and  $\phi_{Zf}$  is the direction cosine between the space-fixed  $Z$  axis and the  $g$ -principal inertial axis. For most chlorine containing molecules the first three terms, being the only ones to contribute to first order, are sufficient to account for the hyperfine structure. This is the case for most of the transitions of chloroketene.

For several transitions of the various isotopes, however, first order theory cannot account for the quadrupole structure.<sup>14</sup> The most obvious of these are the  $^{35}\text{ClHCCO}$   $Q$  branches  $5_{14}-5_{05}$  and  $6_{15}-6_{06}$ , depicted in Figs. 1(b) and 2(b), respectively. First order theory requires that the splittings of the upper and lower fre-

quency pairs of strong lines of a given transition be equal; in the present case these splittings are clearly unequal. Though similar phenomena have been observed in other spectra,<sup>15</sup> this is to the authors' knowledge one of the largest discrepancies observed in a chlorine-containing molecule.

The unequal splittings of these two transitions arise because the contribution of the fourth term of Eq. (6) is significant. The constant  $\chi_{ab}$  is large (see below). There is, furthermore, a near degeneracy (273.92 MHz) calculated from the rotational and centrifugal distortion constants between the levels  $5_{14}$  and  $6_{06}$ , which can be connected by the term  $\phi_{Za} \phi_{Zb}$ . The quadrupole energies are now best calculated by diagonalizing the complete Hamiltonian. The result is a shift of some of the hyperfine levels, as is depicted in Figs. 1(a) and 2(a). The effects on the transitions are shown in Figs. 1(b) and 2(b), in which the observed quadrupole structure is given in comparison with calculated first order and exact hyperfine patterns. There is also a small difference in the relative intensities of the hyperfine components in the two cases. The calculated intensities in Figs. 1(b) and 2(b) are the first order values; there is clearly a difference between these and the observed intensities, especially for the weak components.

Similar anomalies have been observed for several other transitions. For  $^{35}\text{ClHCCO}$  the same near degeneracy described above also causes distortion of  $7_{17}-6_{06}$ . In addition for this isotope,  $14_{2,12}-15_{1,15}$  is also weakly perturbed, by the near degeneracy of  $14_{2,12}$  and  $15_{1,14}$  (1193.51 MHz apart). In  $^{35}\text{ClDCCO}$  there are two relevant near degeneracies: (i)  $4_{13}$  and  $5_{05}$  (956.50 MHz apart), which results in anomalies in  $4_{13}-4_{04}$  and  $5_{14}$

TABLE I. Spectroscopic constants of chloroketene.

Parameter	$^{35}\text{ClHCCO}$	$^{37}\text{ClHCCO}$	$^{35}\text{ClHCCO}$	$^{37}\text{ClHCCO}$
Rotational constants (MHz)				
$A$	36 159.4073(99) <sup>a</sup>	35 952.857 2(113)	29 200.472 9(176)	29 030.7506 (129)
$B$	3 021.8447(10)	2 951.9297(11)	3 022.740 8(27)	2 952.880 6(17)
$C$	2 784.9385(10)	2 724.2597(11)	2 735.440 0(25)	2 676.654 1(17)
Centrifugal distortion constants (quartic in kHz, sextic in Hz)				
$\Delta_J$	1.544 1(21)	1.494 7(23)	1.495(18)	1.443 7(84)
$\Delta_{JK}$	-105.201(69)	-102.402(64)	-72.27(41)	-70.42(21)
$\Delta_K$	2 737.1(11)	2 702.05(98)	1 410.5(39)	1 389.0(21)
$\delta_J$	0.290 29(9)	0.275 02(14)	0.314 33(95)	0.301 07(47)
$\delta_K$	8.252(32)	7.782(90)	7.27(21)	6.75(18)
$H_J$	0.006 29(16)	0.006 34(28)	0.006 9(31)	0.006 2(13)
$H_{JK}$	0 <sup>b</sup>	0 <sup>b</sup>	0 <sup>b</sup>	0 <sup>b</sup>
$H_{KJ}$	-24.65(55)	-20.92(58)	-16.1(56)	-9.3(25)
$H_K$	841.(23)	694.(21)	477.(150)	217.(73)
$h_J$	0.001 44(3)	0.001 42(8)	0 <sup>b</sup>	0.001 59(31)
$h_{JK}$	0.153(18)	0.102(38)	0.28(16)	0.14(12)
$h_K$	0 <sup>b</sup>	0 <sup>b</sup>	0 <sup>b</sup>	0 <sup>b</sup>
Chlorine nuclear quadrupole coupling constants (MHz)				
$\chi_{aa}$	-47.321(38)	-37.789(72)	-47.904(67)	-37.39(83)
$\chi_{bb} - \chi_{cc}$	-39.052(72)	-30.257(152)	-38.792(90)	-30.42(13)
$\chi_{ab}$ <sup>c</sup>	-56.18(65)	-40 <sup>d</sup>	-60.53(194)	-40.15(306)
Total number of rotational transitions	58	56	31	38
Standard deviation of distortion fit (MHz)	0.036	0.037	0.047	0.031

<sup>a</sup>Numbers in parentheses are one standard deviation in units of the last significant figures.

<sup>b</sup>Constrained to zero.

<sup>c</sup>The fits yield only  $|\chi_{ab}|$ . The sign was deduced using structural considerations.

<sup>d</sup>This value was fixed in the least squares fits.

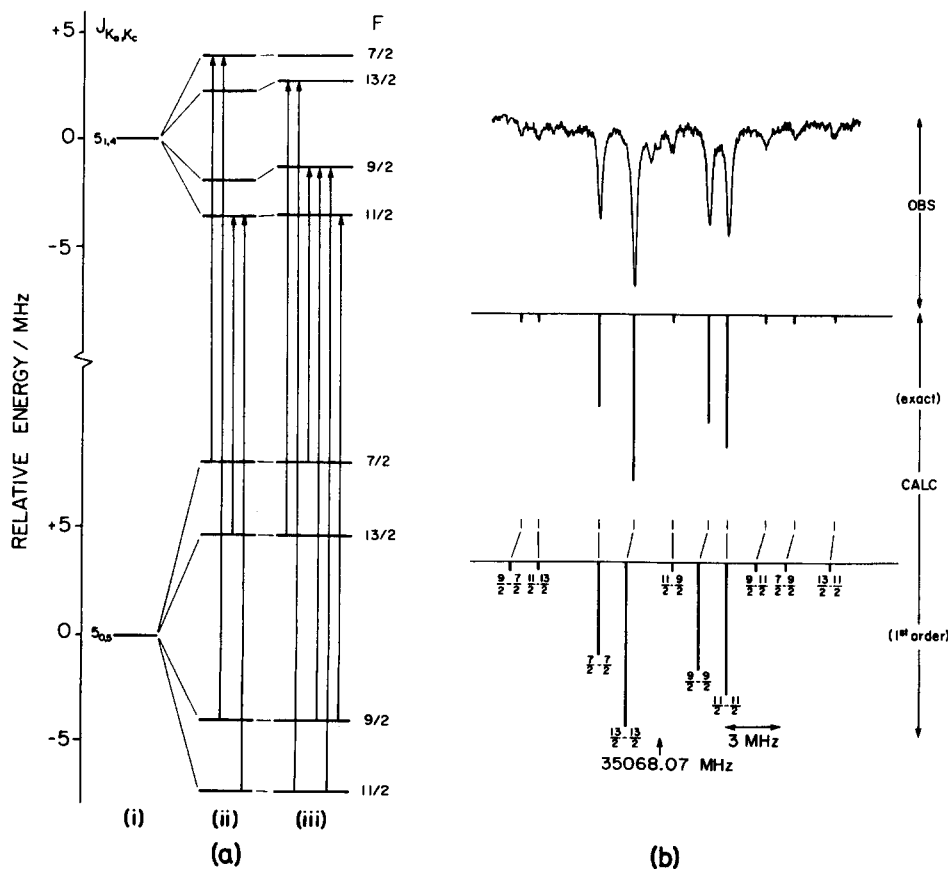


FIG. 1. The  $5_{14}-5_{05}$  transitions of  $^{35}\text{ClHCCO}$  with associated energy levels. (a) The energy levels: (i) The hypothetical unsplit rotational energies; (ii) The chlorine quadrupole energy levels as derived from first order theory, with the unperturbed transitions of (b); (iii) The chlorine quadrupole energy levels as derived from an exact Hamiltonian, with the perturbed transitions of (b). (b) The observed transitions with the calculated first order and exact Hamiltonian patterns.

TABLE II. Observed transition frequencies (in MHz), with hyperfine structure removed, of chloroketene.

Transition	Frequency	Residual <sup>a</sup>
<sup>35</sup> ClHCCO		
1 <sub>1,1</sub> -0 <sub>0,0</sub>	38 941.840	0.009
1 <sub>1,0</sub> -1 <sub>0,1</sub>	33 371.920	-0.005
2 <sub>1,1</sub> -2 <sub>0,2</sub>	33 610.530	0.055
3 <sub>1,2</sub> -3 <sub>0,3</sub>	33 970.690	0.038
4 <sub>1,3</sub> -4 <sub>0,4</sub>	34 455.300	0.028
5 <sub>1,4</sub> -5 <sub>0,5</sub>	35 068.120	0.049
6 <sub>1,5</sub> -6 <sub>0,6</sub>	35 813.680	-0.009
7 <sub>1,6</sub> -7 <sub>0,7</sub>	36 697.580	-0.064
8 <sub>1,7</sub> -8 <sub>0,8</sub>	37 726.230	-0.054
9 <sub>1,8</sub> -9 <sub>0,9</sub>	38 906.730	-0.004
9 <sub>2,8</sub> -10 <sub>1,9</sub>	35 275.120	-0.018
10 <sub>2,9</sub> -11 <sub>1,10</sub>	28 213.720	-0.038
10 <sub>0,10</sub> -9 <sub>1,9</sub>	29 598.700	0.035
11 <sub>0,11</sub> -10 <sub>1,10</sub>	36 358.390	-0.012
12 <sub>0,12</sub> -11 <sub>1,11</sub>	36 531.140	-0.037
13 <sub>0,13</sub> -12 <sub>1,12</sub>	32 900.210	-0.033
16 <sub>0,16</sub> -15 <sub>1,15</sub>	68 887.750	0.066
18 <sub>0,18</sub> -17 <sub>1,17</sub>	58 097.870	-0.038
19 <sub>1,18</sub> -18 <sub>2,17</sub>	31 871.700	0.054
20 <sub>1,19</sub> -20 <sub>0,20</sub>	64 343.150	0.027
20 <sub>3,18</sub> -21 <sub>2,19</sub>	36 788.970	-0.052
21 <sub>3,19</sub> -22 <sub>2,20</sub>	29 626.110	-0.045
22 <sub>3,19</sub> -23 <sub>2,22</sub>	37 533.320	0.012
23 <sub>3,20</sub> -24 <sub>2,23</sub>	32 663.040	0.007
24 <sub>3,21</sub> -25 <sub>2,24</sub>	27 924.230	-0.001
30 <sub>2,28</sub> -29 <sub>3,27</sub>	33 135.390	-0.057
32 <sub>4,29</sub> -33 <sub>3,30</sub>	33 285.630	0.016
33 <sub>4,29</sub> -34 <sub>3,32</sub>	35 453.440	0.015
34 <sub>2,32</sub> -35 <sub>1,35</sub>	28 983.950	0.003
34 <sub>4,30</sub> -35 <sub>3,33</sub>	29 940.610	0.021
35 <sub>2,33</sub> -36 <sub>1,36</sub>	32 616.670	-0.003
36 <sub>2,34</sub> -37 <sub>1,37</sub>	36 567.560	-0.003
38 <sub>5,34</sub> -39 <sub>4,35</sub>	68 893.300	0.003
40 <sub>5,35</sub> -41 <sub>4,38</sub>	58 635.580	0.012
41 <sub>3,38</sub> -40 <sub>4,37</sub>	26 846.980	-0.022
42 <sub>3,39</sub> -41 <sub>4,38</sub>	35 114.100	-0.032
43 <sub>5,39</sub> -44 <sub>4,40</sub>	36 898.980	0.025
44 <sub>5,40</sub> -45 <sub>4,41</sub>	30 274.280	-0.010
44 <sub>5,39</sub> -45 <sub>4,42</sub>	35 023.210	0.037
45 <sub>5,40</sub> -46 <sub>4,43</sub>	29 158.980	0.012
47 <sub>3,45</sub> -46 <sub>4,42</sub>	28 180.020	-0.006
48 <sub>3,46</sub> -47 <sub>4,43</sub>	31 987.960	-0.008
49 <sub>3,47</sub> -48 <sub>4,44</sub>	35 570.850	-0.024
50 <sub>3,48</sub> -49 <sub>4,45</sub>	38 913.240	-0.023
51 <sub>6,45</sub> -52 <sub>5,48</sub>	60 132.060	-0.036
51 <sub>6,46</sub> -52 <sub>5,47</sub>	59 022.360	-0.047
53 <sub>4,49</sub> -52 <sub>5,48</sub>	26 738.940	-0.015
54 <sub>4,50</sub> -53 <sub>5,49</sub>	34 493.780	0.035
55 <sub>6,49</sub> -56 <sub>5,52</sub>	36 098.600	0.024
55 <sub>6,50</sub> -56 <sub>5,51</sub>	33 859.400	-0.012
56 <sub>6,50</sub> -57 <sub>5,53</sub>	30 085.230	0.010
56 <sub>4,53</sub> -55 <sub>5,50</sub>	27 182.530	0.052
56 <sub>6,51</sub> -57 <sub>5,52</sub>	27 441.060	-0.001
57 <sub>4,54</sub> -56 <sub>5,51</sub>	32 426.730	0.061
62 <sub>7,55</sub> -63 <sub>6,58</sub>	62 475.920	0.020
63 <sub>4,60</sub> -62 <sub>5,57</sub>	61 244.080	-0.033
65 <sub>4,62</sub> -64 <sub>5,59</sub>	69 545.720	0.032
74 <sub>5,70</sub> -73 <sub>6,67</sub>	68 872.560	-0.017
<sup>37</sup> ClHCCO		
1 <sub>1,1</sub> -0 <sub>0,0</sub>	38 674.550	-0.081
4 <sub>1,3</sub> -4 <sub>0,4</sub>	34 266.750	0.050
5 <sub>1,5</sub> -4 <sub>0,4</sub>	59 797.720	-0.010
7 <sub>1,6</sub> -7 <sub>0,7</sub>	36 418.120	-0.013
8 <sub>1,7</sub> -8 <sub>0,8</sub>	37 404.030	-0.026

TABLE II (Continued)

Transition	Frequency	Residual <sup>a</sup>
<sup>37</sup> ClHCCO		
9 <sub>1,8</sub> -9 <sub>0,9</sub>	38 534.760	-0.036
9 <sub>2,8</sub> -10 <sub>1,9</sub>	36 403.760	-0.005
10 <sub>0,10</sub> -9 <sub>1,9</sub>	28 264.880	-0.006
10 <sub>2,9</sub> -11 <sub>1,10</sub>	29 520.590	0.012
11 <sub>0,11</sub> -10 <sub>1,10</sub>	34 864.360	0.055
12 <sub>2,10</sub> -13 <sub>1,13</sub>	37 279.380	-0.025
13 <sub>2,11</sub> -14 <sub>1,14</sub>	33 678.190	0.005
14 <sub>2,12</sub> -15 <sub>1,15</sub>	30 301.990	-0.014
15 <sub>2,13</sub> -16 <sub>1,16</sub>	27 165.030	-0.051
19 <sub>1,18</sub> -19 <sub>0,19</sub>	59 569.420	-0.011
19 <sub>1,18</sub> -18 <sub>2,17</sub>	29 023.680	0.047
21 <sub>3,19</sub> -22 <sub>2,20</sub>	32 392.890	0.007
22 <sub>1,21</sub> -22 <sub>0,22</sub>	70 011.090	0.044
23 <sub>3,20</sub> -24 <sub>2,23</sub>	34 665.600	-0.010
24 <sub>3,21</sub> -25 <sub>2,24</sub>	29 977.810	0.009
30 <sub>2,28</sub> -29 <sub>3,27</sub>	28 412.680	0.022
31 <sub>2,29</sub> -30 <sub>3,28</sub>	36 650.010	-0.000
33 <sub>4,29</sub> -34 <sub>3,32</sub>	38 787.080	0.038
33 <sub>4,30</sub> -34 <sub>3,31</sub>	30 549.790	0.043
34 <sub>2,32</sub> -33 <sub>3,31</sub>	62 106.800	-0.003
35 <sub>4,31</sub> -36 <sub>3,34</sub>	28 001.160	0.015
39 <sub>5,34</sub> -40 <sub>4,37</sub>	68 657.480	-0.037
40 <sub>5,35</sub> -41 <sub>4,38</sub>	62 866.300	0.043
40 <sub>5,36</sub> -41 <sub>4,37</sub>	60 835.600	0.069
41 <sub>5,37</sub> -42 <sub>4,38</sub>	54 636.180	-0.038
42 <sub>3,39</sub> -41 <sub>4,38</sub>	28 611.600	-0.022
43 <sub>3,40</sub> -42 <sub>4,39</sub>	36 732.930	0.042
44 <sub>5,40</sub> -45 <sub>4,41</sub>	35 636.220	0.027
45 <sub>5,40</sub> -46 <sub>4,43</sub>	34 018.820	0.042
45 <sub>5,41</sub> -46 <sub>4,42</sub>	29 147.020	0.012
46 <sub>5,41</sub> -47 <sub>4,44</sub>	28 293.240	-0.023
47 <sub>3,44</sub> -46 <sub>4,43</sub>	70 905.950	-0.043
49 <sub>3,47</sub> -48 <sub>4,44</sub>	32 100.950	-0.025
50 <sub>6,44</sub> -51 <sub>5,47</sub>	71 504.540	-0.042
51 <sub>6,46</sub> -52 <sub>5,47</sub>	64 723.160	-0.054
51 <sub>3,49</sub> -50 <sub>4,46</sub>	38 809.940	0.016
52 <sub>6,46</sub> -53 <sub>5,49</sub>	59 795.640	0.025
54 <sub>4,50</sub> -53 <sub>5,49</sub>	26 656.740	0.023
55 <sub>4,51</sub> -54 <sub>5,50</sub>	34 237.380	0.001
56 <sub>6,51</sub> -57 <sub>5,52</sub>	34 096.400	-0.003
56 <sub>6,50</sub> -57 <sub>5,53</sub>	36 318.250	-0.046
57 <sub>6,51</sub> -58 <sub>5,54</sub>	30 444.460	0.013
57 <sub>6,52</sub> -58 <sub>5,53</sub>	27 828.330	-0.033
58 <sub>4,55</sub> -57 <sub>5,52</sub>	31 839.070	0.034
59 <sub>4,56</sub> -58 <sub>5,53</sub>	36 861.070	-0.031
61 <sub>7,54</sub> -62 <sub>6,57</sub>	75 082.640	-0.032
61 <sub>7,55</sub> -62 <sub>6,56</sub>	74 751.540	0.026
62 <sub>7,56</sub> -63 <sub>6,57</sub>	68 846.040	0.004
63 <sub>7,57</sub> -64 <sub>6,58</sub>	62 919.200	0.013
64 <sub>7,57</sub> -65 <sub>6,60</sub>	57 535.900	-0.011
64 <sub>7,58</sub> -65 <sub>6,59</sub>	56 969.400	0.045
<sup>35</sup> ClDCCO		
1 <sub>1,1</sub> -0 <sub>0,0</sub>	31 934.580	-0.077
2 <sub>1,1</sub> -2 <sub>0,2</sub>	26 753.710	0.056
2 <sub>1,2</sub> -1 <sub>0,1</sub>	37 405.900	0.077
3 <sub>1,2</sub> -3 <sub>0,3</sub>	27 192.910	0.021
4 <sub>1,3</sub> -4 <sub>0,4</sub>	27 786.730	0.038
6 <sub>1,5</sub> -6 <sub>0,6</sub>	29 467.330	-0.013
7 <sub>2,5</sub> -8 <sub>1,8</sub>	38 430.590	-0.031
8 <sub>1,7</sub> -8 <sub>0,8</sub>	31 869.880	-0.061
9 <sub>2,7</sub> -10 <sub>1,10</sub>	30 209.270	0.025
9 <sub>0,9</sub> -8 <sub>1,8</sub>	30 003.470	-0.032
9 <sub>1,8</sub> -9 <sub>0,9</sub>	33 371.230	-0.035
10 <sub>0,10</sub> -9 <sub>1,9</sub>	36 734.460	-0.012
10 <sub>1,9</sub> -10 <sub>0,10</sub>	35 090.260	-0.018
11 <sub>1,10</sub> -11 <sub>0,11</sub>	37 040.930	0.026

TABLE II (Continued)

Transition	Frequency	Residual <sup>a</sup>
<sup>35</sup> CIDCCO		
15 <sub>3,13</sub> -16 <sub>2,14</sub>	34 466.630	-0.007
16 <sub>3,13</sub> -17 <sub>2,16</sub>	36 293.340	-0.019
16 <sub>1,15</sub> -15 <sub>2,14</sub>	31 573.150	0.058
17 <sub>3,14</sub> -18 <sub>2,17</sub>	31 234.870	0.042
24 <sub>4,21</sub> -25 <sub>3,22</sub>	35 336.240	0.006
24 <sub>2,22</sub> -23 <sub>3,21</sub>	26 455.720	-0.067
25 <sub>4,21</sub> -26 <sub>3,24</sub>	34 040.020	0.000
25 <sub>2,23</sub> -24 <sub>3,22</sub>	34 881.380	0.039
25 <sub>4,22</sub> -26 <sub>3,23</sub>	28 602.370	-0.023
33 <sub>5,28</sub> -34 <sub>4,31</sub>	38 415.760	-0.014
33 <sub>5,29</sub> -34 <sub>4,30</sub>	36 075.500	0.043
34 <sub>5,29</sub> -35 <sub>4,32</sub>	32 500.940	-0.012
34 <sub>3,31</sub> -33 <sub>4,30</sub>	31 743.710	-0.002
34 <sub>5,30</sub> -35 <sub>4,31</sub>	29 581.210	-0.036
35 <sub>5,30</sub> -36 <sub>4,33</sub>	26 600.300	0.022
39 <sub>3,37</sub> -38 <sub>4,34</sub>	29 414.710	0.015
40 <sub>3,38</sub> -39 <sub>4,35</sub>	32 901.980	-0.011
<sup>37</sup> CIDCCO		
1 <sub>1,1</sub> -0 <sub>0,0</sub>	31 706.180	0.014
4 <sub>1,3</sub> -4 <sub>0,4</sub>	27 623.880	0.044
5 <sub>1,4</sub> -5 <sub>0,5</sub>	28 348.790	-0.032
6 <sub>1,5</sub> -6 <sub>0,6</sub>	29 236.420	-0.025
7 <sub>1,6</sub> -7 <sub>0,7</sub>	30 296.040	-0.048
8 <sub>2,6</sub> -9 <sub>1,9</sub>	34 750.640	0.003
8 <sub>1,7</sub> -8 <sub>0,8</sub>	31 538.400	-0.029
9 <sub>2,7</sub> -10 <sub>1,10</sub>	30 808.750	-0.036
9 <sub>0,9</sub> -8 <sub>1,8</sub>	28 799.310	-0.005
9 <sub>1,8</sub> -9 <sub>0,9</sub>	32 975.200	-0.045
10 <sub>0,10</sub> -9 <sub>1,9</sub>	35 374.390	0.025
10 <sub>1,9</sub> -10 <sub>0,10</sub>	34 619.130	-0.019
11 <sub>1,10</sub> -11 <sub>0,11</sub>	36 483.280	0.032
12 <sub>1,11</sub> -12 <sub>0,12</sub>	38 580.770	0.054
16 <sub>3,14</sub> -17 <sub>2,15</sub>	29 576.210	0.000
16 <sub>3,13</sub> -17 <sub>2,16</sub>	37 763.210	0.006
16 <sub>1,15</sub> -15 <sub>2,14</sub>	29 161.830	-0.019
17 <sub>1,16</sub> -16 <sub>2,15</sub>	36 857.680	0.036
17 <sub>3,14</sub> -18 <sub>2,17</sub>	32 781.740	0.009
18 <sub>3,15</sub> -19 <sub>2,18</sub>	27 924.370	-0.004
24 <sub>4,21</sub> -25 <sub>3,22</sub>	38 238.430	0.031
25 <sub>4,21</sub> -26 <sub>3,24</sub>	36 610.480	0.033
25 <sub>2,23</sub> -24 <sub>3,22</sub>	30 883.600	0.002
25 <sub>4,22</sub> -26 <sub>3,23</sub>	31 718.620	0.001
26 <sub>4,22</sub> -27 <sub>3,25</sub>	31 118.240	0.002
34 <sub>5,29</sub> -35 <sub>4,32</sub>	36 197.410	-0.024
34 <sub>5,30</sub> -35 <sub>4,31</sub>	33 660.030	-0.004
35 <sub>5,30</sub> -36 <sub>4,33</sub>	30 421.520	-0.021
35 <sub>3,32</sub> -34 <sub>4,31</sub>	34 622.920	-0.022
35 <sub>5,31</sub> -36 <sub>4,32</sub>	27 276.810	-0.023
39 <sub>3,37</sub> -38 <sub>4,34</sub>	26 520.640	-0.033
40 <sub>3,38</sub> -39 <sub>4,35</sub>	30 122.410	0.015
42 <sub>3,40</sub> -41 <sub>4,37</sub>	36 458.590	0.007
43 <sub>6,37</sub> -44 <sub>5,40</sub>	36 486.060	-0.002
43 <sub>6,38</sub> -44 <sub>5,39</sub>	35 277.020	0.002
44 <sub>6,39</sub> -45 <sub>5,40</sub>	29 080.170	0.020
44 <sub>4,40</sub> -43 <sub>5,39</sub>	28 497.210	0.012

<sup>a</sup>Observed frequency minus the frequency calculated using the constants in Table I.

-5<sub>05</sub>, and (ii) 7<sub>16</sub> and 5<sub>24</sub> (134.11 MHz apart), resulting in a weak perturbation of 7<sub>16</sub>-7<sub>07</sub>. For <sup>37</sup>CIDCCO the levels 5<sub>05</sub> and 4<sub>13</sub> (479.52 MHz apart) are similarly affected, resulting in anomalies in the transitions 4<sub>13</sub>-4<sub>04</sub> and 5<sub>14</sub>-5<sub>05</sub>. Although unobserved because of overlap-

ping lines, perturbations of 5<sub>14</sub>-5<sub>05</sub> and 6<sub>15</sub>-6<sub>06</sub> of <sup>37</sup>CIHCCO can be expected because 5<sub>14</sub> and 6<sub>06</sub> are 840.14 MHz apart.

Because so many perturbations have been observed, the quadrupole coupling constants have been evaluated by least squares fits using the exact quadrupole Hamiltonian. The matrix elements of Benz, Bauder, and Gunthard<sup>16</sup> were used in a computer program written especially for this purpose. The program also permits simultaneous fitting to the rotational and centrifugal distortion constants through Eqs. (3), (4), and (5). In the present case, however, to save computer time, the rotational and centrifugal distortion constants were fixed to the values already obtained, and the quadrupole fits were made to  $\chi_{aa}$ , ( $\chi_{bb} - \chi_{cc}$ ), and  $\chi_{ab}$ . Since perturbations were observed for three of the four isotopic species such fits were done for these isotopes; for the fourth (<sup>37</sup>CIHCCO)  $\chi_{ab}$  was estimated from the derived geometry, and then held fixed in the fit. The values of the coupling constants are given in Table I.

The quality of the full matrix fits is demonstrated in Table III, which gives the measured frequencies of several transitions, both perturbed and unperturbed, of <sup>35</sup>CIHCCO. These frequencies were also calculated using the derived constants (in Table I) by two methods: one in which  $\chi_{ab}$  was set to zero (equivalent in this case to a first order calculation), and the other in which its value in Table I was used. The residuals (observed-calculated values) are in Table III, and show clearly that the second calculation accounts better for the data. They also indicate the magnitude and location of the significant contributions of  $\chi_{aa}$  to the hyperfine structure.

## THE STRUCTURE OF CHLOROKETENE

The rotational constants were used to obtain structural information about chloroketene. The deductions were made using the principal moments of inertia derived from Watson's "determinable" parameters<sup>13</sup>; these are given in Table IV. This table also contains the inertial defects of the various isotopes, which are clearly small positive numbers, with little variation with isotopic species. The planarity of the molecule is thus confirmed.

Several attempts were made to evaluate the bond lengths and angles. It became clear fairly quickly that although we have available eight independent rotational constants a definitive structure cannot be obtained from our data. Any reasonable model structure shows both atoms of the CH bond near the *b* axis, and the other C atom near the *a* axis (see Fig. 3). The problem is underlined by the changes in the rotational constant *B* on deuteration; these changes are small and positive, and are hence dominated by vibrational effects. This molecule is almost a textbook case of what can go wrong in a structural study!

Nevertheless, some structural information can be obtained. Of the several options open for using the rotational constants for this purpose, we have chosen the following as perhaps the most reasonable. Both coordinates of Cl and the *b* coordinate of H, in <sup>35</sup>CIHCCO, were obtained using the substitution method.<sup>17</sup> The *a*

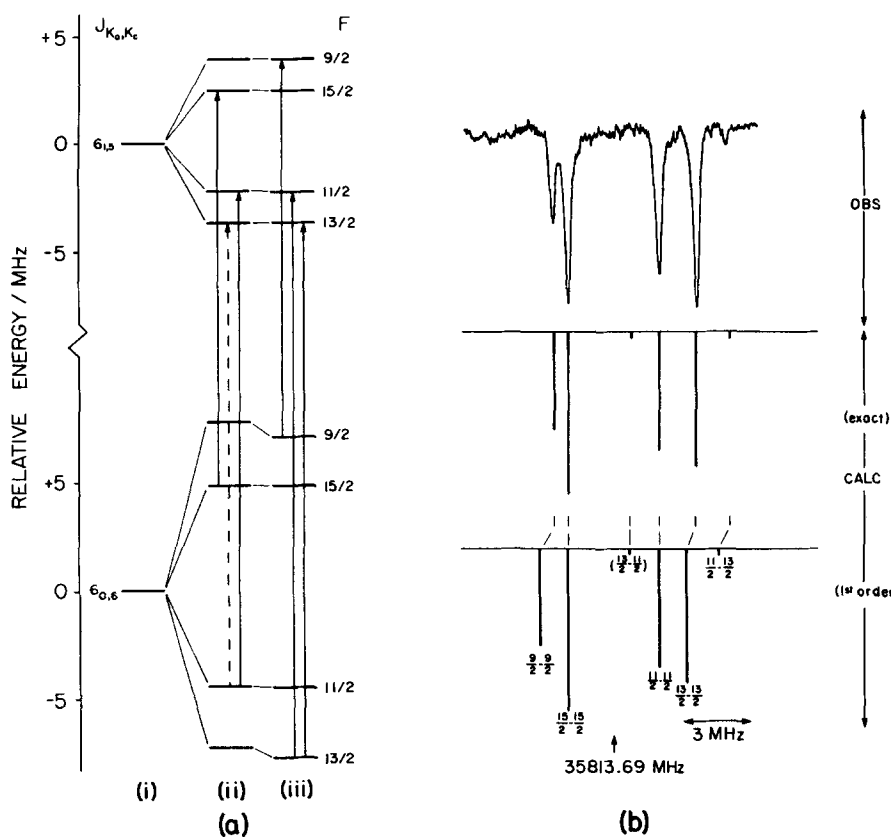


FIG. 2. The  $6_{16}-6_{06}$  transitions of  $^{35}\text{ClHCCO}$  with associated energy levels. (a) The energy levels: (i) The hypothetical unsplit rotational energies; (ii) The chlorine quadrupole energy levels as derived from first order theory, with the unperturbed transitions of (b)—note the omission of the  $13/2-11/2$  transition in the observed spectrum (dashed line); (iii) The chlorine quadrupole energy levels as derived from an exact Hamiltonian, with the perturbed transitions of (b). (b) The observed transitions with the calculated first order and exact Hamiltonian patterns.

coordinate of H was evaluated in several ways. It was, in one case, taken to be zero. In another it was evaluated using the "double substitution" method of Krisher and Pierce<sup>18</sup>; this method, which requires four isotopic species and accurate rotational constants, has been found to give good coordinates in a number of earlier cases,<sup>11,18,19</sup> but has the disadvantage that the *sign* of the coordinate is unavailable. Values of the C=C and C=O lengths were then assumed from ketene<sup>20</sup> and methylketene,<sup>2,3</sup> and, using the various *a* coordinates of H, several different structures were obtained by least squares fits to the observed rotational constants. The CCO angle was fixed in the fits, and was taken to be linear, or bent up to  $8^\circ$  away from the Cl atom, as is found in isoelectronic CINCO.<sup>19</sup> The fits were made to three parameters, chosen to be  $r(\text{C-Cl})$ , and the angles between the *b* axis and the CCl and C=C bonds [ $\angle(\text{Cl-C-b})$  and  $\angle(\text{C=C-b})$ , respectively]. Some resulting structures are given in Table IV.

Although it is clear from Table IV that no definite structure can be derived from our present data, some useful observations can nevertheless be made. The derived parameters [ $r(\text{C-Cl})$ ,  $\angle(\text{Cl-C-b})$ ,  $\angle(\text{C=C-b})$ ] are relatively independent of the assumed C=C and C=O lengths, although they depend fairly strongly on the CCO angle. It seems likely, though, that if the CCO chain is bent this bend is no more than  $1^\circ$  or  $2^\circ$ , because anything larger requires an unacceptably short CH bond (structures IV and V). Plausible CCl bond lengths are obtained in all cases. The angle between the CCl bond and the *b* axis [ $\angle(\text{Cl-C-b})$ ] is surprisingly constant, within  $0.4^\circ$ , in all cases. The HCC and HCCl angles

are essentially indeterminate, with reasonable structures being obtained whether  $a_{\text{H}} = 0$  or  $\pm 0.0745 \text{ \AA}$ ; probably a value of  $127^\circ$  is too big for  $\angle \text{HCCl}$  (structure III), however.

Table V shows a comparison of structures I, II, and VI with those of ketene and methylketene. Clearly all three are reasonable. Any distinction between them cannot be made without further experimental data, such as rotational constants for  $^{13}\text{C}$  and/or  $^{18}\text{O}$ -containing species.

### THE DIPOLE MOMENT

The failure to observe *a*-type transitions was at first surprising, for initial calculations using GAUSSIAN 70

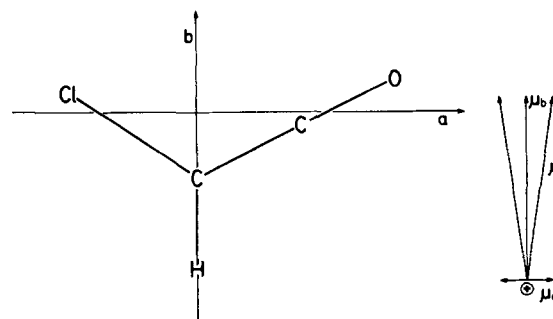


FIG. 3. The atoms of  $^{35}\text{ClHCCO}$  in its principal inertial axis system following structure II (Table IV). At the right the two most likely directions of the dipole moment  $\mu_i$  are given.

TABLE III. Observed hyperfine structure (in MHz) in the microwave spectrum of  $^{35}\text{ClHCCO}$ .

Transition	$F'-F''$	Observed frequency	Residuals	
			$\chi_{ab}$ omitted <sup>a</sup>	$\chi_{ab}$ included <sup>b</sup>
$1_{1,1}-0_{0,0}$	1/2-3/2	38 940.820	0.028	0.019
	3/2-3/2	38 942.630	-0.024	-0.041
	5/2-3/2	38 941.640	0.016	-0.008
$1_{1,0}-1_{0,1}$	5/2-5.2	33 367.420	0.022	0.012
	3/2-1/2	33 368.750	0.023	0.009
	1/2-3/2	33 370.630	0.040	0.023
	3/2-5/2	33 378.280	0.084	0.078
	5/2-3/2	33 379.240	0.014	0.008
$2_{1,1}-2_{0,2}$	7/2-7/2	33 607.430	0.050	0.039
	5/2-5/2	33 618.270	0.052	0.047
$3_{1,2}-3_{0,3}$	3/2-3/2	33 964.360	0.033	0.007
	9/2-9/2	33 968.010	-0.004	-0.019
	5/2-5/2	33 972.300	0.064	0.020
	7/2-7/2	33 975.980	0.048	0.040
$4_{1,3}-4_{0,4}$	5/2-5/2	34 450.480	0.050	0.036
	11/2-11/2	34 452.850	0.045	0.019
	7/2-7/2	34 457.230	0.019	-0.003
	9/2-9/2	34 459.580	-0.011	-0.024
$5_{1,4}-5_{0,5}$	9/2-7/2	35 058.830	0.744	0.065
	11/2-13/2	35 059.920	0.069	0.018
	7/2-7/2	35 063.950	0.048	0.016
	13/2-13/2	35 066.090	0.426	-0.011
	11/2-9/2	35 068.570	0.056	0.013
	9/2-9/2	35 070.780	0.623	-0.020
	11/2-11/2	35 071.970	0.047	-0.019
	9/2-11/2	35 074.280	0.714	0.049
	7/2-9/2	35 075.940	-0.032	-0.029
13/2-11/2	35 078.160	0.425	-0.028	
$6_{1,5}-6_{0,6}$	9/2-9/2	35 810.510	0.635	-0.010
	15/2-15/2	35 811.280	-0.011	0.012
	11/2-11/2	35 815.860	-0.010	-0.017
	13/2-13/2	35 817.680	0.392	-0.038
	11/2-13/2	35 819.090	0.339	-0.057
$7_{1,6}-7_{0,7}$	11/2-11/2	36 694.000	-0.030	0.005
	17/2-17/2	36 695.190	-0.034	-0.025
	13/2-13/2	36 699.820	-0.084	-0.060
	15/2-15/2	36 700.990	-0.110	-0.081
$7_{1,7}-6_{0,6}$	15/2-13/2	70 640.840	0.464	0.031
	13/2-11/2	70 640.840	0.049	0.005
	17/2-15/2	70 644.360	-0.020	-0.019
	11/2-9/2	70 645.380	0.583	-0.056
$8_{1,7}-8_{0,8}$	13/2-13/2	37 722.740	-0.044	-0.024
	19/2-19/2	37 723.810	-0.017	-0.012
	15/2-15/2	37 728.560	-0.058	-0.038
	17/2-17/2	37 729.580	-0.082	-0.067
$9_{1,8}-9_{0,9}$	15/2-15/2	38 903.290	-0.004	-0.003
	21/2-21/2	38 904.160	-0.067	-0.064
	17/2-17/2	38 909.170	0.027	0.027
	19/2-19/2	38 910.090	0.014	0.025
$9_{2,8}-10_{1,9}$	19/2-21/2	35 273.110	0.016	0.015
	17/2-19/2	35 273.770	0.011	0.005
	21/2-23/2	35 276.570	-0.026	-0.030
	15/2-17/2	35 277.200	-0.062	-0.058
$10_{0,10}-9_{1,9}$	17/2-15/2	29 596.430	0.080	0.063
	23/2-21/2	29 597.150	0.006	0.004
	19/2-17/2	29 600.140	0.055	0.050
	21/2-19/2	29 600.880	0.002	-0.005

TABLE III (Continued)

Transition	$F'-F''$	Observed frequency	Residuals	
			$\chi_{ab}$ omitted <sup>a</sup>	$\chi_{ab}$ included <sup>b</sup>
$14_{2,12}-15_{1,15}$	25/2-27/2	29 503.070	-0.024	-0.023
	31/2-33/2	29 503.770	0.029	-0.047
	27/2-29/2	29 510.440	0.010	-0.065
	29/2-31/2	29 510.980	-0.097	-0.097
$13_{2,11}-14_{1,14}$	23/2-25/2	32 896.320	0.021	0.020
	29/2-31/2	32 896.960	-0.008	-0.022
	25/2-27/2	32 903.390	-0.089	-0.094
	27/2-29/2	32 904.080	-0.068	-0.067
$12_{2,11}-13_{1,13}$	21/2-23/2	36 527.270	-0.007	-0.009
	27/2-29/2	36 527.960	-0.016	-0.024
	23/2-25/2	36 534.280	-0.054	-0.055
	25/2-27/2	36 534.970	-0.063	-0.062

<sup>a</sup>Observed frequency minus the frequency calculated using the first three terms of Eq. (6). This is equivalent in this case to a first order calculation.

<sup>b</sup>Observed frequency minus the frequency calculated using all four terms of Eq. (6).

predicted a significant  $\mu_a$  component. To confirm that  $\mu_a$  is indeed small, the dipole moment of  $^{35}\text{ClHCCO}$  was evaluated by measurement of the Stark shifts under an applied field. The transitions  $1_{11} - 0_{00}$  ( $M=0$ ) and  $4_{13} - 4_{04}$  ( $M=3$  and  $4$ ) were used for the purpose, since their Stark effects were predicted to give good separation of  $\mu_a$  and  $\mu_b$ . The cell was calibrated using OCS, and Muentner's value for its dipole moment.<sup>21</sup>

Although the  $M=0$  component of  $1_{11} - 0_{00}$  was easily measured at several fields, the  $M=3$  and  $4$  components of  $4_{13} - 4_{04}$  could be resolved and measured only with difficulty, because of unresolved quadrupole splitting and interference by neighboring lines. The result was reduced accuracy in the measured values of  $\mu_a$  and  $\mu_b$ . The resulting values are  $\mu_a = 0.3 \pm 0.2$ ,  $\mu_b = 1.1 \pm 0.1$ , and  $\mu_{\text{total}} = 1.2 \pm 0.2$  D.

## DISCUSSION AND CONCLUSIONS

Aside from the UPS studies,<sup>8,9</sup> the present work is the first time chloroketene has been observed in isolation. For both preparative methods chloroketene was the only observed product (although molecules like HCl and CO, observed in the UPS experiments, could not have been detected by our spectrometer). Although both preparations used high temperatures, chloroketene was found predominantly in its ground vibrational state. Nevertheless some transitions of vibrationally excited molecules were observed, but were very weak, suggesting that the molecules, by the time they had reached the microwave cell, were essentially in thermal equilibrium at room temperature.

By monitoring the rotational spectrum when chloroketene was isolated in the waveguide, a lifetime of the order of a few minutes was observed at pressures in the range  $30-60 \mu$ . During such a period the chloroketene rotational lines completely disappeared, to be

TABLE IV. Derived structural parameters of chloroketene.

	<sup>35</sup> ClHCCO	<sup>37</sup> ClHCCO	<sup>35</sup> ClDCCO	<sup>37</sup> ClDCCO		
Watson's determinable parameters <sup>a</sup> (MHz)						
A	36 159.4104	35 952.8602	29 200.4759	29 030.7535		
B	3 021.7255	2 951.8142	3 022.6564	2 952.7989		
C	2 784.8535	2 724.1764	2 735.3859	2 676.6006		
Inertial defects (amu Å <sup>2</sup> ) <sup>b</sup>						
Δ	0.2493	0.2499	0.2518	0.2528		
Substitution coordinates in <sup>35</sup> ClHCCO(Å)						
	$a_{Cl} = -1.4264$		$b_{Cl} = 0.2060$			
	$a_H = \pm 0.0745^c$		$b_H = -1.8313$			
Bond lengths and angles <sup>d</sup> obtained from the least squares fits						
	I	II	III	IV	V	VI
$r(\text{CO})^e$	1.161	1.161	1.161	1.161	1.161	1.171
$r(\text{CC})^e$	1.316	1.316	1.316	1.316	1.316	1.306
$a_H^e$	-0.0745	0	0.0745	0	0	0
$\angle(\text{CCO})^e$	180	180	180	184 <sup>f</sup>	188 <sup>f</sup>	180
$r(\text{CCl})^g$	1.726	1.726	1.726	1.739	1.753	1.728
$\angle(\text{Cl}-\text{C}-b)^g$	56.3	56.3	56.3	56.1	56.0	56.4
$\angle(\text{C}=\text{C}-b)^g$	63.5	63.5	63.5	61.6	59.7	63.5
$r(\text{CH})^h$	1.082	1.079	1.082	1.067	1.056	1.080
$\angle(\text{HCCl})^h$	119.3	123.2	127.2	123.0	122.6	123.0
$\angle(\text{HCC})^h$	120.9	117.0	113.0	119.3	121.8	117.2

<sup>a</sup>Reference 13.<sup>b</sup>Derived from moments of inertia calculated using the determinable parameters.  $\Delta = I_c - I_b - I_a$ .<sup>c</sup>Obtained using the double substitution method (Ref. 18).<sup>d</sup>Bond lengths and coordinates in Å, angles in degrees.<sup>e</sup>These parameters were held fixed in an individual least squares fit. Structures I-V assume the C=O and C=O lengths in ketene; structure VI assumes these lengths in methylketene.<sup>f</sup>Angles greater than 180° show the Cl and O atoms to be *trans*.<sup>g</sup>The fits were made to these parameters.<sup>h</sup>These parameters were calculated from the fitted parameters.

replaced by those of other unidentified species. One product is formaldehyde, and in the presence of HCl there is some evidence for regeneration of the starting acid chloride. The known chemistry of ketenes<sup>7</sup> indicates that dimerization is a favored reaction pathway.

Although several attempts were made to observe  $\alpha$ -type transitions, even after accurate rotational constants had been evaluated, no such transitions were ever observed. This is consistent with the small value of  $\mu_a$  of  $0.3 \pm 0.2$  D. Nevertheless, rotational transitions

have often been observed with  $\mu = \sim 0.3$  D, and it seems likely that  $\mu_a$  for chloroketene may be nearer the lower limit of these values.

It is a pity that more definite internuclear parameters could not be obtained. Further progress could be made if a harmonic force field were known, for then the ground state average ( $r_g$ ) structure could be evaluated.<sup>22,23</sup> However, the vibrational spectrum of chloroketene, necessary to obtain the force field, is as yet unknown. We have begun experiments to measure such a spectrum,

TABLE V. A comparison of structural parameters<sup>a</sup> of chloroketene and other ketenes.

Parameter	I	II	VI	ketene	methylketene (Ref. 3)
$r(\text{CH})$	1.082	1.079	1.080	1.078	1.083
$r(\text{CCl})$	1.726	1.726	1.728	...	...
$\angle(\text{HCCl})$	119.3	123.2	123.0	(122.0) <sup>b</sup>	(123.7) <sup>c</sup>
$\angle(\text{HCC})$	120.9	117.0	117.2	119.0	113.7
$r(\text{C}=\text{C})$	1.316	1.316	1.306	1.316	1.306
$r(\text{C}=\text{O})$	1.161	1.161	1.171	1.161	1.171
$\angle(\text{C}=\text{C}=\text{O})$	180	180	180	180	180

<sup>a</sup>Bond lengths in Å. Angles in degrees.<sup>b</sup>This is the  $\angle(\text{HCH})$  in ketene.<sup>c</sup>This is the  $\angle(\text{C}'\text{CH})$  in methylketene, with C' being the methyl carbon.

TABLE VI. Principal values of chlorine quadrupole coupling tensor (in MHz).

	<sup>35</sup> ClHCCO	<sup>35</sup> ClDCCO	<sup>37</sup> ClDCCO
$\chi_{zz}$	-83.4(10) <sup>a</sup>	-87.6(28)	-61.8(42)
$\chi_{xx}$	40.2(15)	44.3(14)	27.9(19)
$\chi_{yy}(=\chi_{cc})$	43.19(4)	43.35(6)	33.96(7)

<sup>a</sup>Uncertainties are one standard deviation in the last significant figures.

and will report on them in due course.

Despite these reservations, a reasonable picture of the structure of chloroketene in its principal axis system has emerged and is presented, along with the measured dipole moment, in Fig. 3. Since the sign of the dipole moment contributions is not obtained we must surmise the resultant direction. From the bond moment ( $C^+ - O^-$ ) and the small negative charge on Cl it is evident that the dipole is oriented close to the *b* axis with the positive end towards the H atom. Which side of the *b* axis is open to conjecture particularly if  $\mu_a$  is at the lower limit; the two possible directions are shown in Fig. 3.

Measurement of  $\chi_{ab}$  has permitted us to calculate the principal values of the chlorine quadrupole coupling tensor for three of the four isotopic species. These values are given in Table VI as  $\chi_{xx}$ ,  $\chi_{yy}$ , and  $\chi_{zz}$ . The values for <sup>35</sup>ClHCCO are well determined; those for the other species are less so. The agreement between the values for the two <sup>35</sup>Cl species is reasonable: to within two standard deviations. Also the ratios of the values for the <sup>35</sup>Cl and <sup>37</sup>Cl species follow the ratios of their respective quadrupole moments, again within two standard deviations.

The diagonalization of the quadrupole tensor also yields the angles between the principal quadrupole axes and the inertial axes. For <sup>35</sup>ClHCCO the angle  $\Theta_{zb}$  between the quadrupole *z* axis, and the *b*-inertial axis, is 57.30 (13)°, where the uncertainty is one standard deviation. This is within one degree of  $\angle(Cl-C-b)$ , the angle between the CCl bond and the *b* axis; the CCl bond is thus essentially the *z*-principal quadrupole axis. Although  $\angle(Cl-C-b)$  seems to be consistent from structure to structure (Table IV), it is not clear, at this stage, given the limitations of the structural calculations, that the difference in angle is meaningful.

The similarity of the values of  $\chi_{xx}$  and  $\chi_{yy}$  implies that the CCl bond is essentially cylindrically symmetrical. This is very consistent with the orbital populations obtained from the STO-3G *ab initio* calculation.<sup>12</sup> The

calculated coupling constants are  $\chi_{zz} = -85.29$ ,  $\chi_{xx} = 43.18$ , and  $\chi_{yy} = 42.12$  MHz, in excellent agreement with the experimental values in Table VI.

## ACKNOWLEDGMENTS

M. C. L. G. thanks the Natural Sciences and Engineering Research Council of Canada for support in the form of Research Grants. W. L-B. acknowledges gratefully the Isaak Walton Killam Foundation for the award of a Fellowship. We thank R. W. Davis for critically reading the manuscript.

- B. E. Turner, *Astrophys. J.* **213**, L75 (1977).
- B. Bak, D. Christensen, J. J. Christiansen, L. Hansen-Nygaard, and J. Rastrup-Andersen, *Spectrochim. Acta* **18**, 1421 (1962).
- B. Bak, J. J. Christiansen, K. Kunstmann, L. Nygaard, and J. Rastrup-Andersen, *J. Chem. Phys.* **45**, 883 (1966).
- W. H. Fletcher and W. B. Barish, *Spectrochim. Acta* **21**, 1647 (1965).
- K. P. R. Nair, H. D. Rudolph, and H. Dreizler, *J. Mol. Spectrosc.* **48**, 571 (1973).
- W. T. Brady, *Synthesis* **1971**, 415.
- The Chemistry of Ketenes, Allenes and Related Compounds*, edited by Saul Patai (Wiley, New York, 1974), Part 1.
- D. Colbourne, D. C. Frost, C. A. McDowell, and N. P. C. Westwood, *Chem. Commun.* **1980**, 250.
- H. Bock, T. Hirabayashi, and S. Mohmand, *Chem. Ber.* **114**, 2595 (1981).
- D. Kivelson, E. B. Wilson, Jr., and D. R. Lide, Jr., *J. Chem. Phys.* **32**, 205 (1960).
- See, for example, W. Gordy and R. L. Cook, *Microwave Molecular Spectra in Technique of Organic Chemistry*, edited by A. Weissberger (Wiley, New York, 1970), Vol. 9, Part 2.
- W. J. Hehre, W. A. Latham, R. Ditchfield, M. D. Newton, and J. A. Pople, *GAUSSIAN 70*, *QCPE* **11**, 236 (1973).
- J. K. G. Watson, in *Vibrational Spectra and Structure, A Series of Advances*, edited by J. R. Durig (Elsevier, New York, 1977), Vol. VI, pp. 1-89.
- C. Flanagan and L. Pierce, *J. Chem. Phys.* **38**, 2963 (1963).
- See, for example, Y. Kikuchi, E. Hirota, and Y. Morino, *Bull. Chem. Soc. Jpn.* **34**, 348 (1961); J. A. Howe, *J. Chem. Phys.* **34**, 1247 (1961).
- H. P. Benz, A. Bauder, and Hs. H. Gunthard, *J. Mol. Spectrosc.* **21**, 156 (1966).
- C. C. Costain, *J. Chem. Phys.* **29**, 864 (1958).
- L. C. Krisher and L. Pierce, *J. Chem. Phys.* **32**, 1619 (1980).
- W. H. Hocking, M. L. Williams, and M. C. L. Gerry, *J. Mol. Spectrosc.* **58**, 250 (1975).
- P. D. Mallinson and L. Nemes, *J. Mol. Spectrosc.* **59**, 470 (1976).
- J. S. Muentzer, *J. Chem. Phys.* **48**, 4544 (1968).
- T. Oka and Y. Morino, *J. Mol. Spectrosc.* **8**, 9 (1962).
- V. W. Laurie and D. R. Herschbach, *J. Chem. Phys.* **37**, 1687 (1962).